MICROSTRUCTURAL STABILITY OF STRONG 9–12 wt% Cr STEELS

H. K. D. H. Bhadeshia
University of Cambridge, Materials Science and Metallurgy
www.msm.cam.ac.uk/phase–trans

Proceedings of *Super–High Strength Steels,* 2–4 November 2005, Rome, Italy, Associazione Italian di Metallurgica, pp. 1–10.

ABSTRACT

The time scales over which an electricity generating plant has to operate reliably are much greater than those available for the development of new alloys, most of which are based on martensitic starting microstructures. The implementation of new alloys is therefore a major risk given that these materials will not have been subjected to tests consistent with extended service. There are two ways of mitigating the risk. Firstly to use the principles of thermodynamics to achieve microstructural stability and secondly to develop better methods for the extrapolation of short–term experimental data. Both of these techniques are discussed in this paper.

INTRODUCTION

There are two themes to this paper. In the first part we shall examine from a purely thermodynamic viewpoint, the factors determining the long–term (10^5 h) stability of martensitic creep–resistant steels. The second part focuses on the methods that should be used to extrapolate short–term data in alloy–design procedures. Although the paper deals with the martensitic steels, its conclusions are general – for this reason it is necessary to briefly explain why martensitic steels are so popular in the modern power generation industry.

For reasons associated with magnetic properties, body–centred cubic iron has the great advantage that its thermal expansion coefficient is low and thermal conductivity high when compared with austenitic steels [1]. These properties permit ferritic alloys to resist thermal fatigue when implemented in thick sections for the construction of power plant, even though the austenitic variants may be stronger in creep. There are many microstructures which are based on the body–centred cubic structure: ferrite, bainite, martensite and a variety of variants of these phases.

Low–chromium steels, such as the classical $2\frac{1}{4}$Cr1Mo or 1CrMoV alloys have formed the backbone of the power generation and petrochemical industries for at least five decades, for operating temperatures of 565°C or less. The $2\frac{1}{4}$Cr1Mo is essentially bainitic. More modern steels such as the 9Cr1Mo martensitic alloys are designed for even higher service temperatures. But why are they martensitic?

The probable answer to this has little to do with microstructure. A greater chromium concentration is needed to obtain the oxidation and corrosion resistance necessary for the greater service temperatures. The chromium must then be balanced by other solutes to avoid an excessive fraction of δ–ferrite. The net solute content then becomes so large that the steels cannot transform to bainite and hence the martensitic microstructure [2]. The martensite *per se* is therefore a *consequence* rather than a design feature. Indeed, it is known that the carbide–precipitation behaviour is not siginificantly different when comparing fully bainitic and fully martensitic microstructures in the same steel [2].

EQUILIBRIUM THERMODYNAMICS AND STABILITY

A good way to examine the long–term stability of a microstructure is by studying its stored energy ΔG_S. We begin with the ΔG_S state of the virgin microstructure before any tempering heat treatment.

Energy can be stored in a material in a large variety of ways [3]. Table 1 compares the calculated stored energies of some elementary microstructures relative to an equilibrium mixture of ferrite, cementite and graphite. The phases in cases 1 and 2 involve the partitioning of all elements so as to minimise free energy. In cases 3-5, the iron and substitutional solutes are configurationally frozen (for martensite even the interstitial elements are frozen). Case 6 refers to an iron-base mechanically alloyed oxide-dispersion strengthened sample which to my knowledge, has the highest reported stored energy prior to recrystallisaton [4]. The magnitudes of the free energy changes as the sytem approaches equilibrium are seen to be very small, but creep-resistant steels have to last for very long time periods, so even these small changes are of importance. Thus, Abe and co-workers have adopted a novel approach in which they design steels where the initial grain structure and precipitate size is very coarse, and have shown that this can lead to creep rupture lives comparable to microstructures where the initial scale is very fine [5, 6].

It is obvious from Table 1 that microstructures with the greatest ΔG_S are the least stable, for example, the virgin martensite is known to be the most unstable phase.

The rate at which a microstructure changes will naturally be greater when the stored energy is large, but account must also be taken of the barriers to achieving equilibrium. Kinetics play an important role and there has been considerable recent research on understanding the interactions between complicated precipitation reactions [7]. Thus, it has been demonstrated that the precipitation of $M_{23}C_6$ can be accelerated by many orders of magnitude, by a subtle change in the overall chemical composition [8, 9]. Both the precipitation and dissolution of metastable precipitates is crucial in predicting these changes [8, 9].

Phase Mixture in Fe–0.2C–1.5Mn wt% at 300 K	Stored Energy / J mol^{-1}
1. Ferrite, graphite & cementite	0
2. Ferrite & cementite	70
3. Paraequilibrium ferrite & paraequilibrium cementite	385
4. Bainite and paraequilibrium cementite	785
5. Martensite	1214
6. Mechanically alloyed ODS metal	55

Table 1: The stored energy as a function of microstructure, relative to the equilibrium state defined as a mixture of ferrite, cementite and graphite. The phases in cases 1 and 2 involve a partitioning of all elements so as to minimise free energy. In cases 3–5 the iron and substitutional solutes are configurationally frozen (for martensite even the interstitial elements are frozen). Case 6 refers to an iron–base mechanically alloyed oxide–dispersion strengthened sample which to my knowledge is the highest reported stored energy prior to recrystallisation [4].

An analysis, based on the components of the free energy stored in a material is useful in other respects, for example in indicating the rate at which certain phases precipitate. A case in hand is $NF616$, a successful martensitic creep–resistant steel, with chemical composition as in Table 2.

C	Mn	Cr	Mo	Ni	V	Nb	W
0.106	0.45	8.96	0.47	–	0.20	0.069	1.83

Table 2: Typical chemical composition, wt%, of $NF616$.

Fig. 1 shows the calculated components of the stored free energy (ΔG_S) of $NF616$. The stored energy is highest when nothing has precipitated so it is not surprising that tempering leads to the rapid precipitation of cementite with an accompanying large reduction in ΔG_S. A further large reduction is achieved by the precipitation of M_2X and $M_{23}C_6$ but only minor reductions when nitrides (MX) and Laves phases are precipitated. It is therefore expected that Laves phase precipitation will be very slow, Fig. 2. Those phases which lead to the smallest reductions in the stored energy of virgin martensite represent the most stable components of the microstructure – these are the components which have to be relied on to contribute to the very long–term creep strength of the steel. After all, the particles which precipitate rapidly are likely to have coarsened well before 10^5 h of service life is achieved.

Statement 1: The long–term stability of creep–resistant steels requires a small rate at which stored free–energy is released. Steels containing a smaller stored energy at the point of service are likely to better maintain their properties during prolonged service at elevated temperatures.

It is also worth examining the *thermodynamic stabilities* of the precipitates which strengthen steels. Cottrell [11] has been able to explain many of the observed trends in the stability, crystal structure and stoichiometry of the carbides of transition metals in terms of chemical bonds. He points out that Ti, Zr and Hf, which in the periodic table are elements near the beginning of the long periods, form very stable MC carbides but the affinity for carbon diminishes further along the rows of the

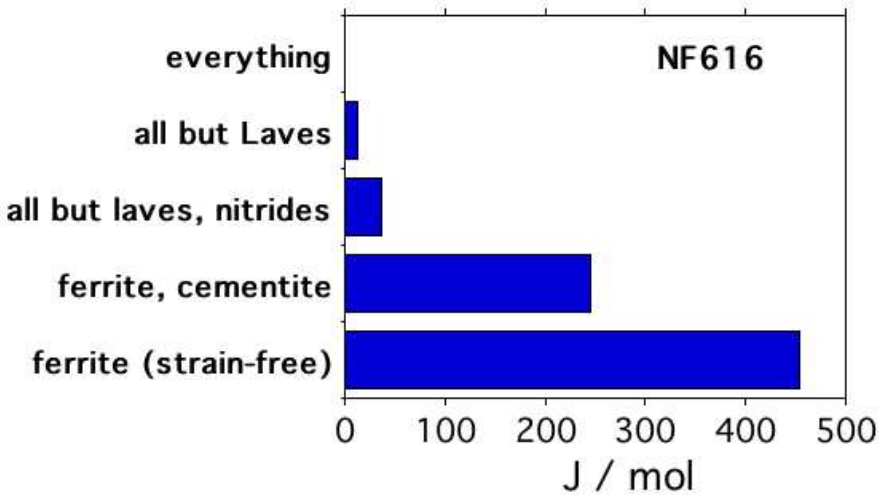

Figure 1: Different contributions to the stored free energy in $NF616$.

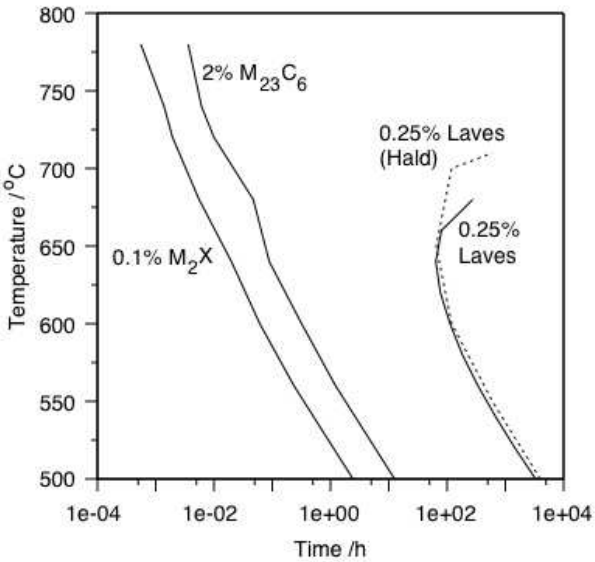

Figure 2: Estimated time temperature transformation diagram for $NF616$.

periodic table, Fig. 3. A part of the reason for this is that more electrons have to be accommodated for elements further along the rows, so antibonding states are progressively filled thereby reducing the bond order. This does not completely explain the trend because the maximum bond order occurs with Cr, Mo and W and we know that carbides of these elements are less stable.

With MC carbides, the metal has to sacrifice four electrons to form the bonds with carbon. Titanium has exactly the right number so that its d–orbitals are left empty on forming TiC. This is not the case with VC, since vanadium has an additional d–electron which forms a V–V bond.

The electrons in the two kinds of bonds, V–C and V–V mutually repel, leading to a reduction in the stability of VC when compared with TiC. This problem becomes larger along the row of the periodic table until MC carbide formation becomes impossible or unlikely.

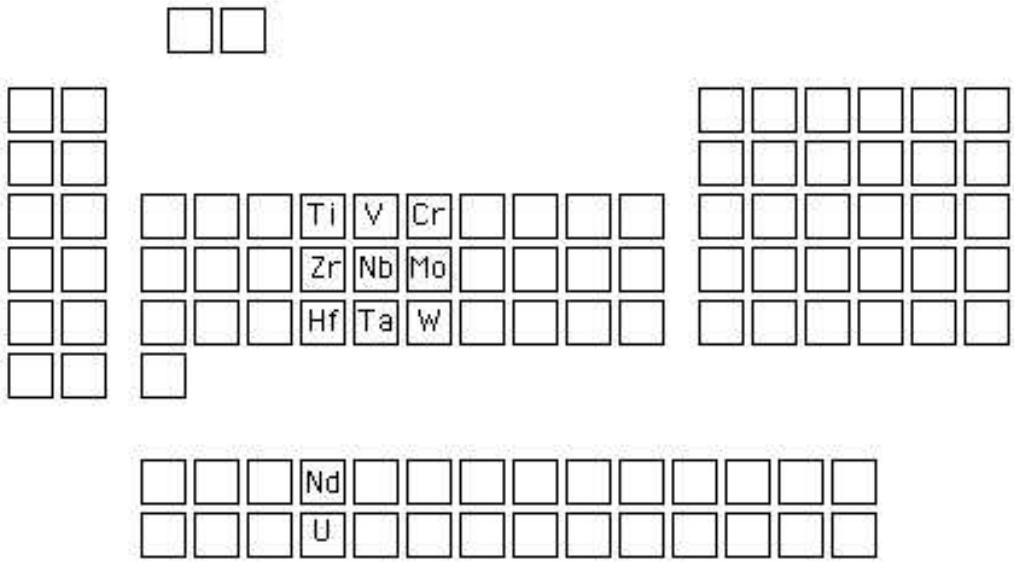

Figure 3: The periodic table showing the positions of strong carbide–forming elements.

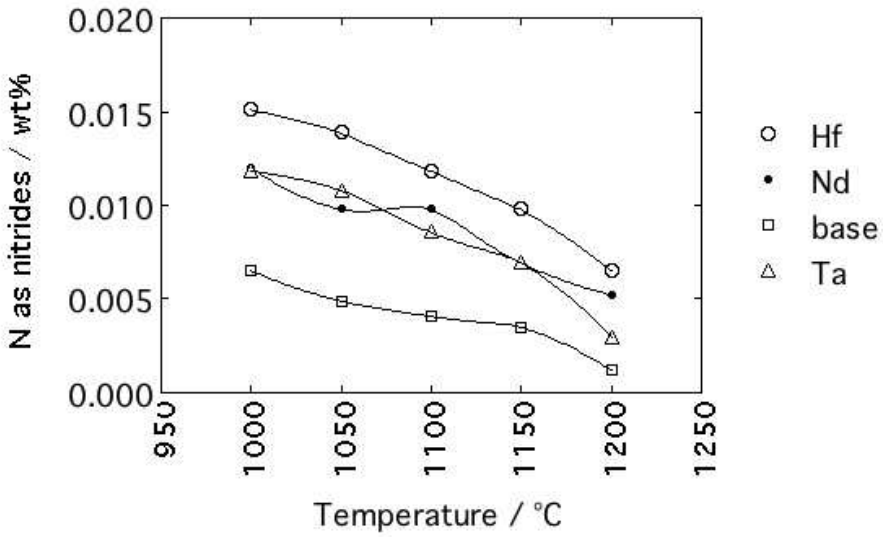

Figure 4: Measured concentration of nitrogen combined in nitrides as a function of the alloying addition to a Fe–0.1C–0.35Si–0.5Mn–9Cr–5Co–3W–0.2V–0.05Nb–0.05N wt% steel. After Igarashi Sawaragi [12].

Although Cottrell has not considered the carbides in the lanthanide or actinide series of elements, it is possible that the same principles apply. Both NdC and UC exist.

The elements also form strong nitrides. Neodynium nitride has already been incorporated into a ferritic creep–resistant steel by Igarashi and Sawaragi [12] with rather good results. The concentration of neodynium used was only 0.04 wt% but gave an increase in the creep rupture life by a factor of about two during tests at 650°C. They also tried hafnium but did not recommend it due to a tendency to form coarse particles.

There is a need for ferritic steels in which any radioactivity induced during service in a nuclear reactor decays rapidly on removal from the radioactive environment. These *reduced activation* alloys are designed without Mo, and Nb, which have long–lived radioactive isotopes. The molybdenum is easily substituted with tungsten. Tantalum behaves in a manner similar to neodynium and niobium, by forming stable nitrides (Fig. 4). It is therefore substituted for niobium in low–activation creep–resistant steels [13].

EXTRAPOLATION AND LONG–TERM PROPERTIES

Mechanical properties are the driving force in all innovation related to steels for elevated temperature applications. We have emphasised that practical creep–resistant materials are complex and hence cannot be adequately designed using simplistic creep model. It is nevertheless important to know the long–term creep and rupture behaviour of such materials for their safe use in safety–critical applications such as power plant and aeroengines. For this reason there exist a large number of empirical or semi–empirical methods, which permit the accurate representation of experimental data and at the same time facilitate the extrapolation of short–term creep data, to varying degrees of success. Many of these methods have been reviewed recently [14, 15]. The following sections describe a few in order to highlight developments in the subject.

Creep strain is a direct measure of remaining life so the safe extrapolation of short–term creep data is a major goal of structural integrity assessment. A popular method involves the use of a θ–parameter equation [16]:

$$\epsilon = \underbrace{\theta_1[1 - \exp\{-\theta_2 t\}]}_{\text{decaying rate}} + \underbrace{\theta_3[\exp\{\theta_4 t\} - 1]}_{\text{accelerating rate}} \tag{1}$$

where θ_i are obtained by fitting to experimental data, and t is the time at temperature. The first two of these parameters describe the primary or decaying strain component, whereas the remaining terms the accelerating regime.

Steady–state creep theory leads to an equation of the form

$$\dot{\epsilon} = a_3 \sigma^n \exp\left\{-\frac{Q}{RT}\right\} \tag{2}$$

where a_3 is an empirical constant. This can be integrated to find the creep rupture time t_r as

$$\ln\{t_r\} = \ln\left\{\frac{\epsilon_r}{a_3}\right\} - n\ln\{\sigma\} + \frac{Q}{RT} \tag{3}$$

Nevertheless, it is found in practice that slightly better fits are obtained by writing [16, 17, 18]:

$$\ln\{t_r\} = a_4 + a_5\sigma + a_6 T \tag{4}$$

where a_i are fitting constants.

Whilst parametric models like these have been applied widely and successfully, they simply are not sufficiently general to deal with large numbers of variables. A more modern technique is the neural network method which thrives in complexity. The method has now been demonstrated to be superior in the extrapolation and representation of creep data. As described below, the neural network method (Bayesian framework) would be a better way of treating creep data with the aim of developing product and design standards than the techniques currently adopted, for example by the European Creep Collaborative Committee [19].

NEURAL NETWORK MODELS

A general method of non–linear regression which avoids the difficulties described above is neural network analysis, as described elsewhere [14]. The details are not discussed here, suffice it to say that there are well–established procedures to avoid overfitting and to give excellent estimates of noise and indeed the uncertainty of creating the model in regions of the input space where data are sparse, noisy or absent. The danger of extrapolation is reduced by a nice treatment of uncertainties.

The neural network can capture interactions between the inputs because it is nonlinear. It can be interrogated to make predictions and to see how these depend on various combinations of inputs.

This methodology has proved to be extremely useful in the analysis of creep phenomena and in structural integrity assessment. The application and success of neural networks in creep have recently been assessed and reviewed [14] with many examples where the number of variables is greater than 50.

Influence of Microstructure

Although the link between microstructure and the creep properties is well–understood for simple systems, the relative importance of the roles of precipitates, solid solution strengthening, microstructure *etc.* in determining the long–term creep rupture properties have not been revealed in the context of applicable alloys.

The neural network method, combined with phase stability calculations, has recently been used to accomplish a non–linear factorisation of the creep–rupture strength into individual components as illustrated in Fig. 5 [20]. It is clear, for example, that the proportion of the contribution to the 10^5 h creep–rupture strength from dissolved solutes increases at 600°C when compared with its role at 500°C. The method is now being used to design microstructures and alloys for their long–term properties. Similar methods have been applied to the nickel–base superalloys.

The National Institute of Materials Science (NIMS) in Japan does an impressive job of measuring and archiving creep data for a large range of materials. These data are made freely available and hence represent a rich source of valuable information. Using these and other published data,

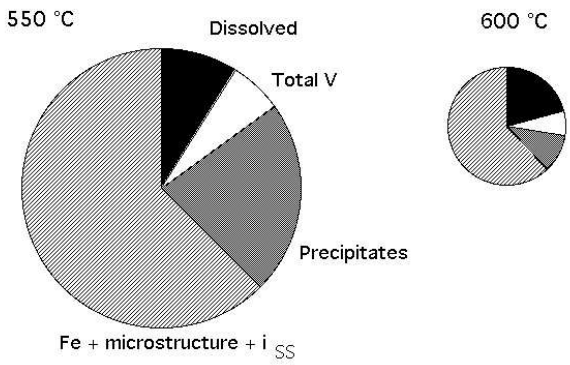

Figure 5: Factorisation of the 10^5 h creep–rupture strength of a $2\frac{1}{2}$Cr1Mo steel at the appropriate temperature. The term i_{SS} represents solid solution strengthening due to elements other than Mo or V. The diameter of each of the pie–charts scales with the creep rupture strength which is 79 and 30 MPa for 550 °C and 600 °C respectively [20].

Sourmail *et al.* created a comprehensive neural network model for the creep rupture strength of austenitic stainless steels, as a function of the chemical composition (16 different elements), the solution treatment temperature, test temperature and time [21]. Much work was carried out to validate the model and to examine its behaviour. However, confidence was boosted when new, long–term creep data were published by NIMS, data which were not included in the creation of the model [22, 23].

Fig.6 illustrates predictions and experimental data (points) for 18Cr–12Ni–Nb austenitic stainless steels [21]. The shaded regions are obtained using the neural network model, the width of the shaded region representing the $\pm 1\sigma$ uncertainties. The curve represents the NIMS prediction using the Orr-Sherby–Dorn method in which the creep rupture data are fitted to an empirical time–temperature parameter using 5th order polynomials. The constant standard error in $\log\{t\}$ was stated to be about 0.102 for steel AEA and 0.154 for steel AEG (t is the time in hours). In the neural network prediction, the uncertainty is not constant but varies depending on where in the input domain the calculations are done. It is clear that the neural network makes better predictions of the unseen long–term data, a fact that is not surprising given that it represents the most general empirical approach.

Statement 2: There is strong fundamental evidence that a well–designed neural network is the best way of extrapolating empirical data. The method should now be more widely exploited in the assessment of creep data.

SUMMARY

In recent years, the focus of alloy design when dealing with creep–resistant steels has rightly shifted from experiments in which claims are made on the basis of short term data to an understanding

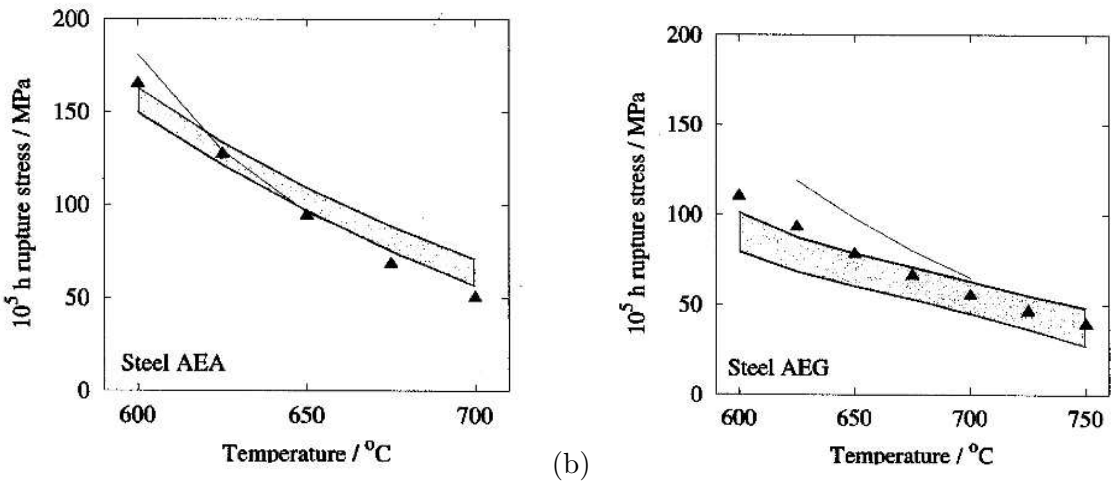

Figure 6: The shaded regions represent neural network model predictions, the curves the NIMS predictions made using the Orr–Sherby–Dorn method. The experimental data were revealed for the two stainless steels after the predictions were made.

of the long–term issues. It is well–known that the initial increments in strength are lost over long periods of time as the microstructure changes during service.

As a general conclusion, it is worth considering the amount of free energy stored inside a steel as a guide to microstructural stability. The relevant stored energy is that present at the point where the steel enters service. Those steels with a smaller stored energy are likely to maintain properties for a longer period of time.

Neural networks are the most generalised methods of regression analysis. This necessarily means that they will be better at extrapolating short–term data in order to design for the longer term. Physical models would be ideal but there are none which can deal with the large number of variables that contribute to the behaviour of the relevant steels.

One difficulty with the concepts discussed in this paper is that they fail to deal with heterogeneities, *i.e.,* local variations which can lead to an overall degradation of properties. These include local recrystallisation due to the presence of coarse carbides at the prior austenite grain boundaries [24] and impurity effects.

References

[1] L. KAUFMAN, E. V. CLOUGHERTY and R. J. WEISS, Acta Metall. 11 (1963) 323–335.

[2] H. K. D. H. BHADESHIA, Proceedings of Ultra–Steel 2000, National Research Insitute for Metals, Tsukuba, Japan (2000) 205–214.

[3] H. K. D. H. BHADESHIA, Materials Science Forum, 284-286 (1998) 39–50.

[4] H. K. D. H. BHADESHIA, Materials Science and Engineering A, A223 (1997) 64–77.

[5] M. IGARASHI, S. MUNEKI AND F. ABE, Key Engineering Materials, 171–175 (2000) 505–512.

[6] K. KIMURA, S. KAZUHIRO, Y. TODA AND F. ABE, ISIJ International, 41 (2001) S121–S125.

[7] J. D. ROBSON and H. K. D. H. BHADESHIA, CALPHAD, 20 (1996) 447–460.

[8] H. K. D. H. BHADESHIA, ISIJ International, 41 (2001) 626–640.

[9] J. D. ROBSON and H. K. D. H. BHADESHIA, Materials Science and Technology, 13 (1997) 631–644.

[10] J. HALD, New Steels for Advanced Plant up to 620 C, EPRI, California, ed. E. Metclafe, (1995) 152–173.

[11] A. H. COTTRELL, Chemical Bonding in Transition Metal Carbides, The Institute of Materials, London (1995) 1–97.

[12] M. IGARASHI and Y. SWARAGI, Proc. Int. Conf. on Power Engineering–97, Japan Society of Mechanical Engineers, Tokyo, Japan (1997) 107–112.

[13] T. HASEGAWA, Y. R. ABE, Y. TOMITA, N. MARUYAMA and M. SAGIYAMA, ISIJ International, 41 (2001) 922–929.

[14] H. K. D. H. BHADESHIA, ISIJ International 39, (1999) 966–979.

[15] M. EVANS, Materials Science and Technology, 15 (1999) 647–658.

[16] R. W. EVANS and B. WILSHIRE, Creep of Metals and Alloys, The Institute of Metals, London (1985).

[17] B. J. CANE, Metal Science, 13 (1981) 287–294.

[18] S. M. BEECH, D. J. GOOCH and A. STRANG, Third International Charles Parsons Conference on Materials Engineering in Turbines and Compressors, Newcastle–upon–Tyne, U. K., (1995) 277–291.

[19] S. R. HOLDSWORTH and G. MERCKLING, 6th International Charles Parsons Turbine Conference, Engineering Issues in Turbine Machinery, Power Plant and Renewables, eds A. Strang, R. D. Conroy, W. M. Banks, M. Blackler, J. Leggett, G. M. McColvin, S. Simplson, M. Smith, F. Starr and R. W. Vanstone, Institute of Materials, London, (2003) 411–426.

[20] M. MURUGANATH and H. K. D. H. BHADESHIA, Mathematical Modelling of Weld Phenomena 6, eds H. Cerjak and H. K. D. H. Bhadeshia, Maney Publishers, London, (2002) 243–260.

[21] T. SOURMAIL, H. K. D. H. BHADESHIA and D. J. C. MACKAY, Materials Science and Technology, 18, (2002) 655–663.

[22] NIMS, Creep Data Sheet 28A, 18Cr–12Ni–Nb Stainless Steel (1983) 1–12.

[23] NIMS, Creep Data Sheet 28B, 18Cr–12Ni–Nb Stainless Steel (2001) 1–25.

[24] K. KIMURA, H. KUSHIMA, F. ABE and K. YAGI, Materials Science and Engineering, A234–236 (1997) 1079–1082.